First Examples of Dinickel Complexes Containing the $N_3Ni(\mu_2\text{-}SR)_3NiN_3$ Core. Synthesis and Crystal Structures of $[L_2Ni_2][BPh_4]_2$ and $[L_3Ni_2][BPh_4]_2$ (L = 2,6-Di(aminomethyl)-4-*tert*-butyl-thiophenolate)

Berthold Kersting*,† and Dieter Siebert‡

Institut für Anorganische und Analytische Chemie and Institut für Physikalische Chemie, Universität Freiburg, Albertstrasse 21, D-79104 Freiburg, Germany

Received February 5, 1998

A coordinatively unsaturated dinuclear Ni^{II} complex of the tridentate ligand 2,6-di(aminomethyl)-4-*tert*-butylthiophenol (HL) has been synthesized and investigated in the context of ligand binding and oxidation state changes. The starting complex $[L_2Ni_2][BPh_4]_2$ (**1**) is readily prepared from NaL, $NiCl_2{\cdot}6H_2O$, and $NaBPh_4$ in methanol. Compound $\mathbf{1}{\cdot}CH_3CN{\cdot}CH_3OH$ crystallizes from an acetonitrile/methanol mixed-solvent system in monoclinic space group $P2_1/n$ with $a = 21.940(4)$ Å, $b = 13.901(3)$ Å, $c = 23.918(5)$ Å, $\beta = 110.00(3)°$, and $Z = 4$. The structure consists of dinuclear $[L_2Ni_2]^{2+}$ cations with two distorted planar *cis*-N_2S_2Ni coordination units joined by the thiophenolate sulfur atoms. The molecule has idealized C_{2v} symmetry. Complex **1** readily adds another 1 equiv of HL to afford the pale green complex $[L_3Ni_2]Cl$ (**2**). The dinuclear structure and its formulation as a 3:2 complex (six-coordinate Ni ions) is derived from UV spectroscopy, cyclic voltammetry, and single-crystal X-ray diffraction of its oxidation product, $[L_3Ni_2]^{2+}$. The dication was prepared by chemical oxidation of **2** with iodine in DMF and isolated as the dark brown BPh_4^- salt, $[L_3Ni_2][BPh_4]_2{\cdot}CH_3OH$ (**3**), which crystallizes in monoclinic space group $P2_1/c$ with $a = 23.678(5)$ Å, $b = 20.090(4)$ Å, $c = 16.797(3)$ Å, $\beta = 106.16(3)°$, and $Z = 4$. Complex **3** is the first structurally characterized example that features a bioctahedral $N_3Ni(\mu_2\text{-}SR)_3NiN_3$ core. Distortions from D_{3h} symmetry suggest that **3** is a trapped-valence $Ni^{II}Ni^{III}$ compound. The Ni−S and Ni−N bond lengths vary from 2.2975(9) to 2.4486(12) Å and from 2.027(3) to 2.120(3) Å, respectively. On the CV time scale complex **2** undergoes two reversible electron-transfer reactions at $E_{1/2} = -0.02$ and $+0.44$ V vs SCE, affording **3** and the transient dark green trication $[L_3Ni_2]^{3+}$ ($\tau_{1/2} \approx 15$ min at 295 K), respectively. While **2** is EPR silent, the EPR spectrum of a powdered sample of **3** reveals $g_\perp = 4.0$ and $g_\parallel = 2.09$ at 77 K, consistent with an $S = {}^3/_2$ spin state of the mixed-valent $Ni^{II}Ni^{III}$ complex.

Introduction

Dinuclear thiolate-bridged metal complexes of the 3d transition metals have come under increased investigation in the past several years because such assemblies occur in the active sites of many enzymes.[1−4] Consequently, the structural, magnetic, spectroscopic, and redox properties of numerous dinuclear complexes of mono- or bidentate thiolate ligands have been the focus of interest. However, these reactions often require exact stoichiometric control, without which the reaction mixture may contain species of different nuclearity.[5−7] Furthermore, an investigation of chemical reactivities is often hampered by the fact that nickel or iron thiolate complexes can be notoriously labile. Additionally, these may undergo ligand-based oxidation with the result of decomposition of such species.[8−10]

Of more recent origin is the development of binuclear systems obtained by using binucleating linear[11] or bis-macrocyclic N,S-donor ligands.[12,13] The notable feature of such complexes is their kinetic stability that enables the molecules to cycle between high and low formal metal oxidation states.[14] Furthermore, binding of exogenous ligands does not affect the dinuclear structure.[13] Unfortunately, these ligands are not readily available

* Author to whom correspondence should be addressed (e-mail: kerstber@sun2.ruf.uni-freiburg.de).
† Institut für Anorganische und Analytische Chemie.
‡ Institut für Physikalische Chemie.

(1) (a) Kaim, W.; Schwederski, B. *Bioanorganische Chemie*, 2nd ed.; Teubner Studienbücher Chemie: Stuttgart, 1995. (b) Lippard, S. J.; Berg, J. M. *Principles of Bioinorganic Chemistry*; University Science Books: Mill Valley, 1994.
(2) Volbeda, A.; Charon, M.-H.; Piras, C.; Hatchikian, E. C.; Frey, M.; Fontecilla-Camps, J. C. *Nature* **1995**, *373*, 580−7.
(3) Iwata, S.; Ostermeier, C.; Ludwig, B.; Michel, H. *Nature* **1995**, *376*, 660−9.
(4) Tsukihara, T.; Aoyama, H.; Yamashita, E.; Tomizaki, T.; Yamaguchi, H.; Shinzawa-Itoh, K.; Nakashima, R.; Yaono, R.; Yoshikawa, S. *Science* **1995**, *269*, 1069−74.
(5) Krebs, B.; Henkel, G. *Angew. Chem.* **1991**, *105*, 785−804; *Angew. Chem., Int. Ed. Engl.* **1991**, *30*, 769−88.
(6) Dance, I. G. *Polyhedron* **1986**, *5*, 1037−104.
(7) Blower, P. J.; Dilworth, J. R. *Coord. Chem. Rev.* **1987**, *76*, 121−85.
(8) Krüger, H.-J.; Holm, R. H. *Inorg. Chem.* **1989**, *28*, 1148−55.
(9) Kumar, M.; Day, R. O.; Colpas, G. J.; Maroney, M. J. *J. Am. Chem. Soc.* **1989**, *111*, 5974−6.
(10) Oxidation of nickel(II) thiolate complexes to sulfenate, sulfinate, and sulfonate complexes has also been reported: (a) Farmer, P. J.; Solouki, T.; Mills, D. K.; Soma, T.; Russell, D. H.; Reibenspies, J. H.; Darensbourg, M. Y. *J. Am. Chem. Soc.* **1992**, *114*, 4601−5. (b) Mirza, S. A.; Day, R. O.; Maroney, M. J. *Inorg. Chem.* **1996**, *35*, 1992−5. (c) Font, I.; Buonomo, R.; Reibenspies, J. H.; Darensbourg, M. Y. *Inorg. Chem.* **1993**, *32*, 5897−8. (d) Buonomo, R. M.; Font, I.; Maguire, M. J.; Reibenspies, J. H.; Tuntulani, T.; Darensbourg, M. Y. *J. Am. Chem. Soc.* **1995**, *117*, 963−73. (e) Henderson, R. K.; Bouwman, E.; Spek, A. L.; Reedijk, J. *Inorg. Chem.* **1997**, *36*, 4616−7.
(11) (a) Murase, I.; Ueno S.; Kida, S. *Bull. Chem. Soc. Jpn.* **1983**, *56*, 2748−51. (b) Lawrance, G. A.; Maeder, M.; Manning, T. M.; O'Leary, M. A.; Skelton, B. W.; White, A. H. *J. Chem. Soc., Dalton Trans.* **1990**, 2491−5.

S0020-1669(98)00131-1 CCC: $15.00
Published on Web 07/07/1998

and often require multistep reactions. Thus, only a few examples of dimetallic Ni, Cu, and Zn complexes of tridentate N_2S and macrocyclic hexadentate N_4S_2 ligands have been characterized to date.[11−15]

For nickel, the tridentate N_2S and hexadentate N_4S_2 ligands produce almost exclusively planar N_2S_2Ni complexes that feature a central $Ni(\mu_2\text{-}SR)_2Ni$ core,[11,13] similar to that seen in complexes of mono- or bidentate thiolate ligands.[16] Some complexes have been reported to readily bind substrates axially.[13a,g] However, an occupation of the vacant third bridge position by exogenous ligands to yield a $Ni(\mu_2\text{-}SR)_3Ni$ core has not been observed. It should be noted that dinuclear nickel complexes that feature such a triple thiolate bridge are rare. To the best of our knowledge, the $Ni(\mu_2\text{-}SR)_3Ni$ core was first encountered in the bitetrahedral complex $[(RS)Ni(\mu_2\text{-}SR)_3Ni(SR)]^-$ (R = 2,4,5-$Pr^i_3C_6H_2$).[17] Similar bitetrahedral structures were previously reported for $[Co_2(SR)_5]^-$ (R = isopropyl)[18] and subsequently in $[Fe_2(SR)_5]^-$ (R = *tert*-butyl).[19] The compound $[Ni\{Co(aet)_3\}_2]^{2+}$ (aet = 2-aminoethanethiolate) contains a trinuclear $N_3Co(\mu_2\text{-}SR)_3Ni(\mu_2\text{-}SR)_3CoN_3$ core.[20] A triply bridged $Ni(\mu_2\text{-}SR)_2(X)Fe$ structure (X = unknown ligand) also occurs in the active center of the [NiFe]-hydrogenase from *Desulfovibrio gigas*.[21]

We have recently described the synthesis and the electrochemical and magnetic properties of the 3:2 (L:M) dinuclear Fe^{III} and Co^{III} complexes $[L_3M_2]^{3+}$, where L represents the tridentate N_2S ligand 2,6-di(aminomethyl)-4-*tert*-butyl-thiophenol (HL).[22] Now we have succeeded in obtaining the corresponding nickel complexes by reaction of the 2:2 complex $[L_2Ni_2]^{2+}$ with a further 1 equiv of HL. Reported herein are the synthesis and characterization of the first $Ni^{II}Ni^{II}$ and $Ni^{II}Ni^{III}$ complexes featuring the $N_3Ni(\mu_2\text{-}SR)_3NiN_3$ core. We further present the crystal structures of the 2:2 and 3:2 complexes.

Experimental Section

General Information. The ligand $HL\cdot(HCl)_2$ was prepared by reduction of benzyl[2,6-di(hydroximinoformyl)-4-*tert*-butyl-phenyl]-sulfide with sodium in liquid ammonia.[23] All other chemicals were of reagent grade and used without further purification. The solvents were predried over molecular sieves and freshly distilled from appropriate drying agents. The syntheses of metal complexes were performed under an atmosphere of dry nitrogen except where other conditions are mentioned explicitly. Melting points were determined in capillaries and are uncorrected. CHN analyses were determined with a Perkin-Elmer elemental analyzer 240. IR spectra were recorded on a Bruker IFS25 spectrophotometer as KBr pellets. Absorption spectra were recorded on a Jasco V-750 UV/vis/near-IR spectrometer. Cyclic voltammetry measurements were carried out at 25 °C with an EG&G Princeton Applied Research potentiostat/galvanostat model 263 A. The cell contained a Pt working electrode, a Pt wire auxiliary electrode, and a Ag wire as reference electrode. Concentrations of solutions were 0.1 M in supporting electrolyte ($Bu^n_4NPF_6$) and ca. 1×10^{-3} M in sample. Ferrocenium/ferrocene was used as internal standard. All potentials were converted to the SCE reference.[24] Coulometric experiments were performed with the use of a Pt-gauze electrode. EPR spectra were recorded by a conventional Varian X-band spectrometer with 100 kHz modulation.

Preparation of Complexes. $[L_2Ni_2][BPh_4]_2$ (1). To a solution of $HL\cdot(HCl)_2$ (595 mg, 2.00 mmol) in methanol (10 mL) was added 2.00 mL of a 1.00 M solution of $NiCl_2\cdot6H_2O$ in methanol (2.00 mmol). The resulting pale yellow solution was stirred for a further 10 min. Then a 12 mL portion of a 0.50 M solution of NaOMe in methanol (6.00 mmol) was added. To the dark red solution was added a solution of $NaBPh_4$ (855 mg, 2.50 mmol) in methanol (2 mL) to cause the product to precipitate as a red microcrystalline powder. Filtration and recrystallization from CH_3CN/MeOH (1:1) solution affords the acetonitrile methanol solvate $\mathbf{1}\cdot CH_3CN\cdot CH_3OH$ as dark red crystals. Yield: 0.94 g (74%). Mp: 232−234 °C. Anal. Calcd for $C_{72}H_{78}B_2N_4S_2Ni_2\cdot CH_3CN\cdot CH_3OH$: C, 70.62; H, 6.72; N, 5.49. Found: C, 69.70; H, 6.33; N, 4.88. ^{1}H NMR (CD_2Cl_2, 200 MHz): δ 7.57 (s br, 16 H, Ar*H*), 7.10 (m, 28 H, Ar*H*), 3.37 (s, 3 H, C*H*$_3$OH), 3.19 (d, J = 12 Hz, 4 H, C*H*$_2$), 2.62 (t, J = 12 Hz, 4 H, C*H*$_2$), 1.97 (s, 3 H, C*H*$_3$CN), 1.31 (s, 18 H, C*H*$_3$), 0.51 (d, J = 12 Hz, 4 H, N*H*$_2$), −0.03 (t, J = 12 Hz, 4 H, N*H*$_2$). ^{13}C NMR (CD_2Cl_2, 50.3 MHz): δ 164.0 (q, $^1J(^{11}BC)$ = 49 Hz), 152.7, 135.6, 135.2, 128.3, 126.9, 123.1, 121.9, 117.7, 50.1, 45.8, 34.9, 30.8, 1.7.

$[L_2Ni_2][ClO_4]_2$ (1′). This compound was prepared by a procedure similar to that described for **1**. $Ni(ClO_4)_2\cdot6H_2O$ (731 mg, 2.00 mmol) was used instead of $NiCl_2\cdot6H_2O$ and $LiClO_4\cdot3H_2O$ (802 mg, 5.00 mmol) instead of $NaBPh_4$. A red microcrystalline material was isolated by filtration, dried in air, and recrystallized from MeOH. Yield: 0.43 g (57%). **Caution!** *Transition-metal perchlorates are hazardous and may explode. Only small quantities should be prepared and great care taken.*[25] Anal. Calcd for $C_{24}H_{38}N_4S_2Ni_2Cl_2O_8$: C, 37.78; H, 5.02; N, 7.34. Found: C, 37.69; H, 5.00; N, 7.30. IR (KBr, cm^{-1}): $\tilde{\nu}$ 1105 ($\nu_3(F_2)$ ClO_4^-).

$[L_3Ni_2]Cl$ (2). To a solution of **1** (128 mg, 0.100 mmol) in acetonitrile (7 mL) was added a solution of $HL\cdot(HCl)_2$ (30 mg, 0.101 mmol) in methanol (1 mL). Addition of 3 drops of NEt_3 caused the precipitation of a pale green solid, which was isolated by filtration and dried in vacuo. This material was recrystallized from ethanol. Yield:

(12) (a) Hughes, J. G.; Robson, R. *Inorg. Chim. Acta* **1979**, *35*, 87−92. (b) Louey, M.; Nichols, P. D.; Robson, R. *Inorg. Chim. Acta* **1980**, *47*, 87−96. (c) Iliopoulos, P.; Murray, K. S.; Robson, R.; Wilson, J. C.; Williams, G. A. *J. Chem. Soc., Dalton Trans.* **1987**, 1585−91. (d) Bond, A. M.; Haga, M.; Creece, I. S.; Robson, R.; Wilson, J. C. *Inorg. Chem.* **1989**, *28*, 559−66. (e) Hoskins, B. F.; McKenzie, C. J.; Robson, R.; Zhenrong, L. *J. Chem. Soc., Dalton Trans.* **1990**, 2637−41. (f) Hoskins, B. F.; Robson, R.; Williams, G. A.; Wilson, J. C. *Inorg. Chem.* **1991**, *30*, 4160−6.

(13) (a) Atkins, A. J.; Blake, A. J.; Schröder, M. *J. Chem. Soc., Chem. Commun.* **1993**, 1662−5. (b) Brooker, S.; Croucher, P. D. *J. Chem. Soc., Chem. Commun.* **1995**, 1493−4. (c) Brooker, S.; Croucher, P. D. *J. Chem. Soc., Chem. Commun.* **1995**, 2075−6. (d) Atkins, A. J.; Black, D.; Blake, A. J.; Marin-Becerra, A.; Parsons, S.; Ruiz-Ramirez, L; Schröder, M. *J. Chem. Soc., Chem. Commun.* **1996**, 457−64. (e) Brooker, S.; Croucher, P. D.; Roxburgh, F. M. *J. Chem. Soc., Dalton Trans.* **1996**, 3031−7. (f) Branscombe, N. D. J.; Blake, A. J.; Marin-Becerra, A.; Li, W.-S.; Parsons, S.; Ruiz-Ramirez, L.; Schröder, M. *J. Chem. Soc., Chem. Commun.* **1996**, 2573−4. (g) Brooker, S.; Croucher, P. D. *J. Chem. Soc., Chem. Commun.* **1997**, 459−60.

(14) For mononuclear complexes of macrocyclic N,S-donor ligands with metal ions in high formal oxidation states, see: (a) Sellmann, D.; Emig, S.; Heinemann, F. W. *Angew. Chem.* **1997**, *109*, 1808−10; *Angew. Chem., Int. Ed. Engl.* **1997**, *36*, 1734−6. (b) Sellmann, D.; Emig, S.; Heinemann, F. W.; Knoch, F. *Angew. Chem.* **1997**, *109*, 1250−2; *Angew. Chem., Int. Ed. Engl.* **1997**, *36*, 1201−3. (c) Hanss, J.; Krüger, H.-J. *Angew. Chem.* **1996**, *108*, 2989−91; *Angew. Chem., Int. Ed. Engl.* **1996**, *35*, 2827−30. (d) Hanss, J.; Krüger, H.-J. *Angew. Chem.* **1998**, *110*, 366−9; *Angew. Chem., Int. Ed. Engl.* **1998**, *37*, 360−3.

(15) Beissel, T.; Glaser, T.; Kesting, F.; Wieghardt, K.; Nuber, B. *Inorg. Chem.* **1996**, *35*, 3936−47.

(16) Halcrow, M. A.; Christou, G. *Chem. Rev.* **1994**, *94*, 2421−81.

(17) Silver, A.; Millar, M. *J. Chem. Soc., Chem. Commun.* **1992**, 948−9.

(18) Henkel, G.; Weissgräber, S. *Angew. Chem.* **1992**, *104*, 1382−3; *Angew. Chem., Int. Ed. Engl.* **1992**, *31*, 1368−9.

(19) Henkel, G.; Chen, C. *Inorg. Chem.* **1993**, *32*, 1064−5.

(20) Konno, T.; Okamoto, K.-I.; Hidaka, J. *Acta Crystallogr.* **1993**, *C49*, 222−4.

(21) (a) Volbeda, A.; Garcin, E.; Piras, C.; de Lacey, A. L.; Fernandez, V. M.; Hatchikian, E. C.; Frey, M.; Fontecilla-Camps, J. C. *J. Am. Chem. Soc.* **1996**, *118*, 12989−96. (b) Halcrow, M. A. *Angew. Chem.* **1995**, *107*, 1307−10; *Angew. Chem., Int. Ed. Engl.* **1995**, *34*, 1193−7.

(22) Kersting, B.; Kolm, M. J.; Janiak, C. *Z. Anorg. Allg. Chem.* **1998**, *624*, 775−780.

(23) Kersting, B. *Eur. J. Inorg. Chem.*, in press.

(24) For formal potentials of the ferrocenium/ferrocene couple vs SCE, see: Connelly, N. G.; Geiger, W. E. *Chem. Rev.* **1996**, *96*, 877−910. Under our experimental conditions, the couple ferrocenium/ferrocene (Fc^+/Fc) is at $E_{1/2}$ = 0.45 V (DMF, CH_2Cl_2) and $E_{1/2}$ 0.40 V (CH_3CN) vs Ag.

(25) Wolsey, W. C. *J. Chem. Educ.* **1973**, *50*, A335.

Table 1. Crystal Data and Structure Refinement for **1** and **3**

	1	**3**
empirical formula	$C_{75}H_{85}B_2N_5Ni_2OS_2$	$C_{85}H_{101}B_2N_6Ni_2OS_3$
fw	1275.64	1457.94
cryst size, mm^3	0.30 × 0.50 × 1.20	0.40 × 0.50 × 0.15
T, K	293	213
space group	$P2_1/n$	$P2_1/c$
a, Å	21.940(4)	23.678(5)
b, Å	13.901(3)	20.090(4)
c, Å	23.918(5)	16.797(3)
β, deg	110.00(3)	106.16(3)
V, Å^3	6854(2)	7675(3)
Z	4	4
density, g·cm^{-3}	1.236	1.262
μ(Mo Kα), mm^{-1}	0.657	0.622
θ range, deg	2.93−26.07	4.37−26.01
reflns collected	14 393	54 356
unique reflns	13 460 (R_{int} = 0.0147)	14 892 (R_{int} = 0.1148)
obsd reflns	8937 ($F_o > 4\sigma(F_o)$)	11 240 ($F_o > 4\sigma(F_o)$)
R1, wR2 [$F_o > 4\sigma(F_o)$]	0.0580, 0.1475[a]	0.0504, 0.1202[b]
R1, wR2 (all data)	0.1093, 0.1852[a]	0.0730, 0.1360[b]
goodness-of-fit on F^2	1.16	1.00
resid electron density, e·Å^{-3}	0.791/−0.775	0.604/−0.480

[a] $w = 1/[\sigma^2(F_o^2) + (0.0814P)^2 + 5.84P]$, $P = (F_o^2 + 2F_c^2)/3$. [b] $w = 1/[\sigma^2(F_o^2) + (0.0529P)^2 + 6.41P]$, $P = (F_o^2 + 2F_c^2)/3$.

55 mg (64%). Anal. Calcd for $C_{36}H_{57}N_6S_3Ni_2Cl$·EtOH: C, 52.52; H, 7.31; N, 9.67. Found: C, 52.13; H, 7.67; N, 9.21.

$[L_3Ni_2][BPh_4]_2$ (3). To a solution of **2** (87 mg, 0.10 mmol) in DMF (3 mL) was added a solution of I_2 (13 mg, 0.051 mmol) in DMF (1 mL), and the resulting brown solution was stirred for 20 min. The reaction mixture was allowed to warm to 30 °C, at which temperature it was evaporated to dryness. The resulting black solid was redissolved in methanol (30 mL) and separated from a small quantity of a white solid by filtration. To the brown filtrate was added a solution of $NaBPh_4$ (75 mg, 0.22 mmol) in methanol, and the solution was stored at room temperature for 2 days. The resulting black crystals were collected by filtration and dried in air. Yield: 99 mg (68%). Anal. Calcd for $C_{85}H_{101}N_6B_2ONi_2S_3$: C, 70.03; H, 6.98; N, 5.76. Found: C, 69.76; H, 7.04; N, 5.61.

X-ray Structure Determinations. Single crystals of **1**·CH_3CN·CH_3OH were grown by recrystallization from MeOH/CH_3CN solution. Black crystals of **3**·CH_3OH suitable for single-crystal X-ray determination were obtained by the procedure described above. Reflection data were collected on an Enraf-Nonius CAD4 diffractometer (**1**) or on a STOE IPDS diffractometer (**3**) using Mo Kα radiation (λ = 0.710 73 Å). The data were corrected for Lorentz and polarization effects and for absorption (empirical absorption correction, program XEMP[26]). Crystal parameters and details of the data collection and refinement are summarized in Table 1. The crystal structures were solved by direct methods, and refinements were carried out on F^2 values using SHELXTL software.[26] All non-hydrogen atoms were refined anisotropically except for the carbon atoms of the disordered *tert*-butyl groups. These were refined isotropically. Hydrogen atoms were placed at calculated positions except for the MeOH solvate of **1**. They were refined riding on the corresponding atoms with a common isotropic thermal parameter. The methyl carbon atoms of both *tert*-butyl groups of **1** and of one *tert*-butyl group of **3** are disordered. The multiplicities of the respective orientations (C(31A)−C(33A), C(31B)−C(33B); C(41A)−C(43A), C(41B)−C(43B) (**1**); C(210)−C(212), C(213)−C(215) (**3**)) were refined as follows: 0.53, 0.47; 0.51, 0.49 (**1**); 0.60, 0.40 (**3**).

Results and Discussion

Synthesis and Reactions of Complexes 1−3. The reaction of HL·$(HCl)_2$ with $NiCl_2$·$6H_2O$ and NaOMe in methanol in a 1:1:3 ratio readily affords the dinuclear $[L_2Ni_2]^{2+}$ cation, which was isolated as the air-stable tetraphenylborate salt $[L_2Ni_2][BPh_4]_2$ (**1**) (Scheme 1). Complex **1** is a dark red crystalline solid, soluble in polar aprotic solvents like acetonitrile, methylene chloride, dimethyl sulfoxide, and dimethylformamide. When recrystallized from acetonitrile/methanol solution, it is obtained as the solvate **1**·CH_3CN·CH_3OH. The dinuclear structure of the $[L_2Ni_2]^{2+}$ cation in **1**·CH_3CN·CH_3OH was confirmed by single-crystal X-ray diffraction (*vide infra*).

Scheme 1

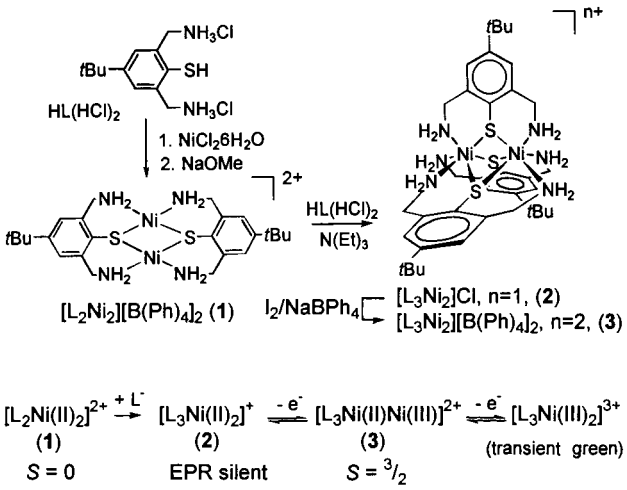

Though **1**·CH_3CN·CH_3OH is diamagnetic in the solid state, a discrete ^{1}H NMR spectrum could only be obtained for a CD_2Cl_2 solution of a sample that had been thoroughly dried in vacuo. Suprisingly, the resonances of the CH_2 and NH_2 goups (four multiplets of equal intensity in the 2.5 to −0.1 ppm region) are still observed at relatively high field,[27] presumably due to a paramagnetic species. Since the deuterated solvent contained traces of water, these upfield shifts are probably due to rapid exchange of Ni-bound and free water molecules. It appears that the solid state structure is only retained in noncoordinating solvents, whereas in CD_3OD or CD_3CN solution the absence of the expected CH_2NH_2 resonances in the 0−10 ppm region indicates binding of solvent molecules to the dimetal centrum to yield a paramagnetic species.

The ability of complex **1** to bind substrates is further demonstrated by the facile reaction with another 1 equiv of HL. When a solution of **1** in acetonitrile is treated with 1 equiv of HL, an immediate color change from dark red to pale green is observed. The color change is accompanied by formation of a pale green solid that analyzes as $[L_3Ni_2]Cl$ (**2**). Although structural data is yet not available for **2**, the $[L_3Ni_2]^+$ cation is assumed to be isostructural to its oxidation product $[L_3Ni_2]^{2+}$ in $[L_3Ni_2][BPh_4]_2$ (**3**). The structure of **3** has been determined by X-ray crystallography. Further support comes from cyclic voltammetry, infrared spectroscopy, and UV/vis spectroscopy.

Complex **2** is an air-sensitive compound. Exposure of solutions of **2** in methanol to air results in a color change from pale green to dark brown. Alternatively, these brown solutions are also produced by chemical oxidation of **2** with 0.5 equiv of iodine or bromine. In contrast to **2**, complex **3** is stable in air

(26) Sheldrick, G. M. *SHELXS-86*; University of Göttingen: Göttingen, Germany, 1990. Sheldrick, G. M. *SHELXL-93*; University of Göttingen, Göttingen, Germany, 1993.

(27) For example, the similar pattern of C*H*$_2$ and N*H*$_2$ resonances (4 multiplets) observed for the corresponding diamagnetic Pd complex $[L_2Pd_2][BPh_4]_2$ appears in the region 5.47−3.42 ppm. ^{1}H NMR (DMSO-d_6, 200 MHz): δ 7.44 (s, 4H, Ar*H*), 7.20−7.14 (m, 16H, Ar*H*), 6.96−6.75 (m, 24H, Ar*H*), 5.47 (d, J = 12 Hz, 4H, C*H*$_2$), 4.50 (t, J = 12 Hz, 4H, C*H*$_2$), 4.05 (d, J = 12 Hz, N*H*$_2$), 3.42 (t, J = 12 Hz, N*H*$_2$), 1.25 (s, 18H, C*H*$_3$).

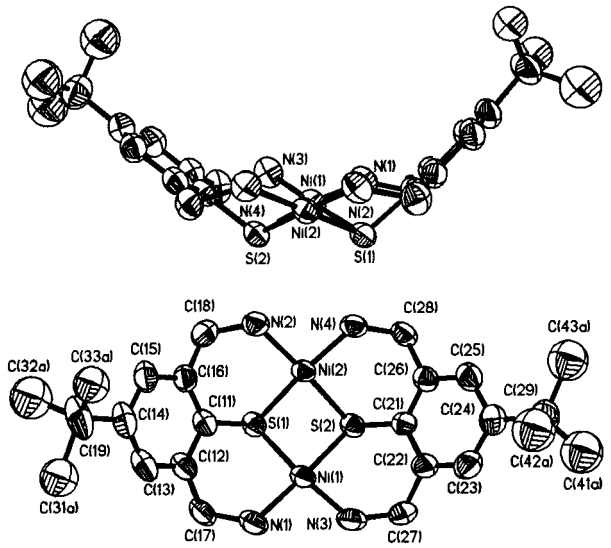

Figure 1. Perspective views (top, side view; bottom, view along the pseudo C_2 axis) of the molecular structure of the dication in **1** (50% probability thermal ellipsoids). Hydrogen atoms are omitted for clarity. Only one orientation of the disordered *tert*-butyl groups is displayed.

both in the solid state and in solution. As is indicated by UV/vis spectroscopy, oxidation of **2** with I_2 or O_2 affords the same $[Ni_2L_3]^{2+}$ cation. It is also noted that the oxidation of **2** is chemically reversible. Thus, addition of $NaBH_4$ to a solution of **3** reforms $[L_3Ni_2]^+$. Reduction of **3** with Zn in DMF also gives **2**.

Finally, addition of 1.0 or 0.5 equiv of I_2 to DMF solutions of **2** or **3**, respectively, results in the formation of a transient dark green solution. The lifetime of the species produced on oxidation is, however, long enough to allow for its characterization by UV/vis spectroscopy. Here, the dark green color is tentatively assigned to the species $[L_3Ni_2]^{3+}$, which is thermally unstable. In accord with these chemical transformations are the CV experiments presented below, which clearly indicate that reactions 1a and 1b are one-electron-transfer processes.

$$[L_3Ni_2]^+ + {}^1/_2I_2 \rightarrow [L_3Ni_2]^{2+} + I^- \qquad (1a)$$

$$[L_3Ni_2]^{2+} + {}^1/_2I_2 \rightarrow [L_3Ni_2]^{3+} + I^- \qquad (1b)$$

Crystal Structure Determinations. Structure of 1·CH_3CN·CH_3OH. The X-ray crystal structure determination of **1**·CH_3CN·CH_3OH revealed the structure to consist of well-separated molecules of the dinickel complex and two tetraphenylborate anions. The two molecules of solvent of crystallization form hydrogen bonds with nitrogen atoms (N(1), N(3)) of the dication (N(1)−H(1B)···O(1) 2.911 Å, N(3)−H(3A)···N(5) 3.353 Å), but feature no bonding interactions with the nickel ions. Perspective views of the dication of **1** are shown in Figure 1; coordination spheres are depicted in Figure 3. Within the dinuclear $[Ni_2L_2]^{2+}$ cation each nickel ion forms one four-membered and two six-membered chelate rings. The two approximately planar *cis*-N_2S_2Ni coordination units are joined by the thiolate sulfur atoms. Maximum deviations from the least-squares planes defined by the atoms Ni(1), S(1), S(2), N(1), N(3) and Ni(2), S(1), S(2), N(2), N(4) are 0.08 and 0.02 Å, respectively. The structures of the two tetraphenylborate anions and solvent molecules are unexceptional and are not further considered.

The dication possesses idealized C_{2v} symmetry and has a bowl-shaped molecular structure that is best described by angles

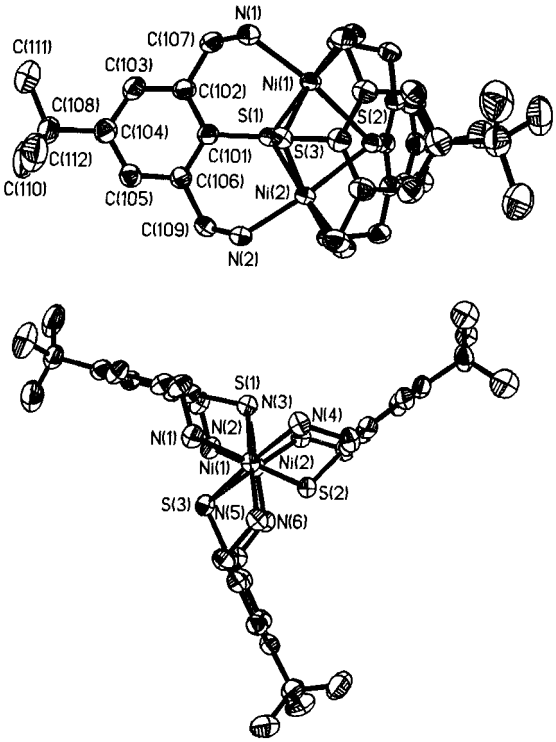

Figure 2. Perspective views (top, side view; bottom, view along the pseudo C_3 axis) of the molecular structure of the dication in **3** (50% probability thermal ellipsoids). Hydrogen atoms are omitted for clarity. Only one orientation of the disordered *tert*-butyl group (C(210)−C(212)) is displayed.

of 124.6° and 96.1° between the two square planes defined by the two N_2S_2 arrays and the phenyl rings of the ligands. A similar folding of two N_2S_2Ni planes at the thiolate sulfur atoms has been observed for a series of dinickel complexes of macrocyclic imine−thiophenolate ligands, however, with a less distinct curvature.[13] Accordingly, a shorter Ni···Ni separation of 2.973(1) Å is seen in **1**. The average Ni−S and Ni−N bond lengths of 2.182 and 1.936 Å, respectively, closely compare with those reported for Ni^{II} complexes containing planar Ni-(N_2S_2)[28] and $NiN_2(\mu_2\text{-}SR)_2$[11b] structures. Compared to other planar N_2S_2Ni amine−thiolate complexes, there are no unusual structural features, other than a less rigid ligand topology and sterically less encumbered ligands, that would favor binding of further substrates in **1**.

Structure of 3·CH_3OH. The X-ray crystal structure determination of **3**·CH_3OH revealed the structure to consist of discrete, dinuclear $[Ni_2L_3]^{2+}$ complex cations in which two *fac*-N_3S_3Ni units are joined by the thiolate sulfur atoms. The dication possesses idealized D_{3h} symmetry. Hence the dication exists as the meso isomer (Λ,Δ)-$[Ni_2L_3]^{2+}$ in the solid state. Figure 2 displays perspective views (perpendicular and parallel to the pseudo C_3 axis) of the dication in **3**, coordination spheres are depicted in Figure 3, and selected bond lengths and angles are summarized in Tables 2 and 3.

The Ni−N and Ni−S bond lengths are in the range 2.027(3)−2.115(3) Å (mean 2.089 Å) and 2.2975(9)−2.4486(12) Å (mean 2.380 Å). It is noted that deviations in Ni−N and Ni−S bond lengths appear to be larger at Ni(2). Thus, deviation in Ni−N bond lengths at Ni(1) is at 0.048 Å, whereas at Ni(2) a value of 0.088 Å is observed. Similarly, deviation in Ni(1)−S

(28) (a) Mill, D. K.; Reibenspies, J. H.; Darensbourg, M. Y. *Inorg. Chem.* **1990**, *29*, 4364−6. (b) Yamamura, T.; Tadokoro, M.; Tanaka, K.; Kuroda, R. *Bull. Chem. Soc. Jpn.* **1993**, *66*, 1984−90.

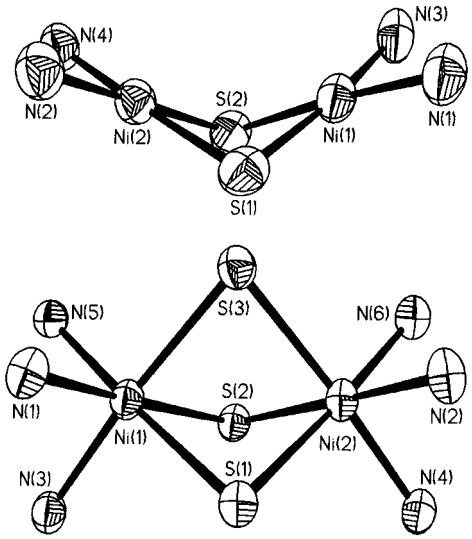

Figure 3. Coordination units in the central $N_2Ni(\mu_2\text{-}SR)_2NiN_2$ (top) and $N_3Ni(\mu_2\text{-}SR)_3NiN_3$ cores (bottom) in **1** and **3**, respectively, showing 50% thermal ellipsoids and atom-numbering schemes. Bond lengths and angles are collected in Tables 2 and 3.

Table 2. Selected Bond Lengths (Å) for $[L_2Ni_2][BPh_4]_2\cdot CH_3CN\cdot CH_3OH$ (**1**) and $[L_3Ni_2][BPh_4]_2\cdot CH_3OH$ (**3**)

		1	
Ni(1)−S(1)	2.189(1)	Ni(2)−S(1)	2.187(1)
Ni(1)−S(2)	2.183(1)	Ni(2)−S(2)	2.182(1)
Ni(1)−N(1)	1.930(3)	Ni(2)−N(2)	1.936(3)
Ni(1)−N(3)	1.939(3)	Ni(2)−N(4)	1.939(3)
S(1)−C(11)	1.779(4)	S(2)−C(21)	1.774(4)
Ni(1)···Ni(2)	2.973(1)	S(1)···S(2)	2.828(1)
		3	
Ni(1)−N(1)	2.072(3)	Ni(2)−N(2)	2.027(3)
Ni(1)−N(3)	2.120(3)	Ni(2)−N(4)	2.115(3)
Ni(1)−N(5)	2.085(2)	Ni(2)−N(6)	2.113(3)
Ni(1)−S(1)	2.3773(9)	Ni(2)−S(1)	2.3632(10)
Ni(1)−S(2)	2.3593(9)	Ni(2)−S(2)	2.2975(9)
Ni(1)−S(3)	2.4486(12)	Ni(2)−S(3)	2.4370(9)
S(1)−C(101)	1.764(3)	C(207)−N(3)	1.480(4)
S(2)−C(201)	1.757(3)	C(209)−N(4)	1.480(4)
S(3)−C(301)	1.775(3)	C(307)−N(5)	1.481(4)
C(107)−N(1)	1.493(4)	C(309)−N(6)	1.486(4)
C(109)−N(2)	1.493(4)		
Ni(1)···Ni(2)	3.064(1)	S(1)···S(3)	3.278(1)
S(1)···S(2)	3.066(1)	S(2)···S(3)	3.122(1)

bond lengths (0.089 Å) is smaller than at Ni(2) (0.140 Å). The longest Ni−N bonds (Ni(1)−N(3), Ni(2)−N(4)) are observed trans to the longest Ni−S bonds (Ni(1)−S(3), Ni(2)−S(3)). These longer bonds may be the result of a Jahn−Teller distortion (vide infra). In contrast to the deviations in the bond lengths, the respective bond angles at Ni(1) and Ni(2) are all very similar (average N−Ni−N, S−Ni−S, *cis*-S−Ni−N, and *trans*-S−Ni−N angles of 90.6°, 83.0°, 93.1°, and 174.3°, respectively).

The longer Ni−N and Ni−S bond lengths in **3** are comparable with those in six-coordinate $N_{6-n}S_nNi^{II}$ complexes, while the shorter Ni−N and Ni−S bond lengths are close to those in six-coordinate $N_{6-n}S_nNi^{III}$ complexes. For example, the longest Ni−N bonds in **3** are nearly equal to the average Ni−N bond length of 2.10 Å reported for the N_6Ni^{II} compound $[NiL_2](NO_3)\text{-}Cl\cdot H_2O$ (L = 1,4,7-triazacyclononane).[29] The shortest Ni−N bond in **3**, on the other hand, comes close to the mean value of 1.971 Å of the four equatorial $Ni-N_{eq}$ bonds in the N_6Ni^{III} complex $[NiL_2](S_2O_6)_3\cdot 7H_2O$ (L = 1,4,7-triazacyclononane).[30]

Table 3. Selected Bond Angles (deg) for $[L_2Ni_2][BPh_4]_2\cdot CH_3CN\cdot CH_3OH$ (**1**) and $[L_3Ni_2][BPh_4]_2\cdot CH_3OH$ (**3**)

		1	
S(1)−Ni(1)−N(1)	95.1(1)	S(1)−Ni(2)−N(2)	95.8(1)
S(1)−Ni(1)−S(2)	80.62(4)	S(1)−Ni(2)−S(2)	80.65(4)
S(1)−Ni(1)−N(3)	173.8(1)	S(1)−Ni(2)−N(4)	175.1(1)
S(2)−Ni(1)−N(1)	174.6(1)	S(2)−Ni(2)−N(4)	94.7(1)
S(2)−Ni(1)−N(3)	95.5(1)	S(2)−Ni(2)−N(2)	176.3(1)
N(1)−Ni(1)−N(3)	89.0(1)	N(4)−Ni(2)−N(2)	88.8(1)
		3	
N(1)−Ni(1)−N(3)	92.46(11)	N(2)−Ni(2)−N(4)	90.53(10)
N(1)−Ni(1)−N(5)	91.35(10)	N(2)−Ni(2)−N(6)	91.21(11)
N(3)−Ni(1)−N(5)	88.60(10)	N(4)−Ni(2)−N(6)	89.40(11)
S(1)−Ni(1)−S(2)	80.66(3)	S(1)−Ni(2)−S(2)	82.25(4)
S(1)−Ni(1)−S(3)	85.54(3)	S(1)−Ni(2)−S(3)	86.11(3)
S(2)−Ni(1)−S(3)	80.95(3)	S(2)−Ni(2)−S(3)	82.44(3)
N(1)−Ni(1)−S(1)	93.40(7)	N(2)−Ni(2)−S(1)	92.97(8)
N(1)−Ni(1)−S(2)	172.34(7)	N(2)−Ni(2)−S(2)	174.14(8)
N(1)−Ni(1)−S(3)	93.83(8)	N(2)−Ni(2)−S(3)	93.90(8)
N(3)−Ni(1)−S(1)	92.77(7)	N(4)−Ni(2)−S(1)	92.74(8)
N(3)−Ni(1)−S(2)	92.66(7)	N(4)−Ni(2)−S(2)	93.08(7)
N(3)−Ni(1)−S(3)	173.57(7)	N(4)−Ni(2)−S(3)	175.48(7)
N(5)−Ni(1)−S(1)	174.99(7)	N(6)−Ni(2)−S(1)	175.29(7)
N(5)−Ni(1)−S(2)	94.47(7)	N(6)−Ni(2)−S(2)	93.45(8)
N(5)−Ni(1)−S(3)	92.56(7)	N(6)−Ni(2)−S(3)	91.44(8)

Likewise, the mean Ni−S bond lengths in **3** fall in the middle of the range of Ni^{II}−S and Ni^{III}−S bond lengths in six-coordinate $N_{6-n}S_nNi$ complexes. In *cis*-$[Ni(bpy)_2(SPh)_2]\cdot 2D_2O$[31] and $[Ni(pdtc)_2]^-$ ($pdtcH_2$ = pyridine-2,6-bis(thiocarboxylic acid)),[32] for example, the mean Ni^{II}−S and Ni^{III}−S bond lengths are at 2.44 and 2.28 Å, respectively.

The question arises whether the one-electron oxidation of **2** may be assigned metal- or ligand-centered or whether the unpaired electron is delocalized over the $[L_3Ni_2]^{2+}$ cation. The decrease in Ni−S and Ni−N bonds in **3** relative to those in other six-coordinate $N_{6-n}S_nNi^{II}$ complexes is the effect expected as a consequence of metal-centered oxidation. Furthermore, the individual bond lengths and angles within the three ligands of **3** (average C−C, C−N, and C−S bond lengths of 1.394, 1.486, and 1.765 Å, respectively) show no unusual features and are almost identical to the respective values found in **1** (1.387, 1.489, and 1.777 Å, respectively). This rules out the possibility that one of the three ligands is coordinated as a thiyl radical.[33,34] Such species are expected to exhibit different bond lengths within the ligand framework similarly to transition-metal phenolato/phenoxyl radical complexes.[35] A metal-centered oxidation of **2** is also supported by infrared spectroscopy.

The distortions from ideal D_{3h} symmetry (different metric parameters of the individual *fac*-N_3S_3Ni coordination units) suggest that this complex is a trapped-valence $Ni^{II}Ni^{III}$ complex rather than being delocalized.[36] Such a species would be expected to have structurally identical nickel sites.[37]

(29) Zompa, L. J.; Margulis, T. N. *Inorg. Chim. Acta* **1978**, *28*, L157−9.
(30) Wieghardt, K.; Walz, W.; Nuber, B.; Weiss, J.; Ozarowski, A.; Stratemeier, H.; Reinen, D. *Inorg. Chem.* **1986**, *25*, 1650−4.
(31) Osakada, K.; Yamamoto, T.; Yamamoto, A.; Takenaka, A.; Sasada, Y. *Acta Crystallogr.* **1984**, *C40*, 85−7.
(32) Krüger, H.-J.; Holm, R. H. *J. Am. Chem. Soc.* **1990**, *112*, 2955−63.
(33) (a) Rundel, W. *Z. Naturforsch.* **1960**, *15b*, 546−7. (b) Rundel, W. *Chem. Ber.* **1969**, *102*, 1649−55.
(34) (a) Treichel, P. M.; Rosenhein, L. D. *J. Am. Chem. Soc.* **1981**, *103*, 691−2. (b) Treichel, P. M.; Rosenhein, L. D.; Schmidt, M. S. *Inorg. Chem.* **1983**, *22*, 3960−5.
(35) Sokolowski, A.; Bothe, E.; Bill, E.; Weyermüller, T.; Wieghardt, K. *J. Chem. Soc., Chem. Commun.* **1996**, 1671−2.
(36) It is unlikely that the distortions from ideal D_{3h} symmetry result from steric requirements of the thiolate ligand. The corresponding cobalt complex $[L_3Co^{III}_2]^{3+}$, for example, contains structurally identical Co^{III} sites. Kersting, B.; Volkmer, D. Unpublished results.
(37) Creutz, C. *Prog. Inorg. Chem.* **1985**, *33*, 1−73.

Chart 1

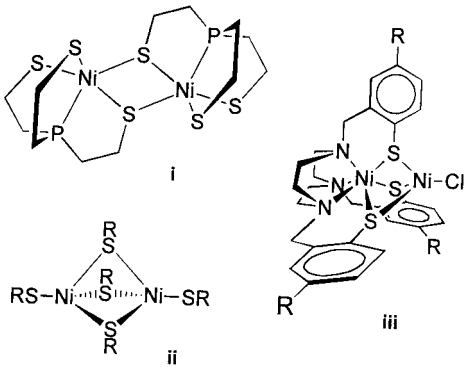

Comparison with Other Structures. Compound **3** is unique because it is a crystallographically characterized mixed-valent nickel(II,III) compound featuring a face-sharing bioctahedral $[N_3Ni(\mu_2\text{-}SR)_3NiN_3]$ core. The structure of $[Ni_2\{P(o\text{-}C_6H_4S)_3\}_2]^-$ represents the only other example for a dinuclear mixed-valent $Ni^{II}Ni^{III}$ thiolate complex (structure **i** in Chart 1).[38] A central $Ni(\mu_2\text{-}SR)_3Ni$ structure occurs in the face-sharing bitetrahedral complex $[(RS)Ni(\mu_2\text{-}SR)_3Ni(SR)]^-$ (structure **ii**, R = 2,4,5-Pr^i_3-C_6H_2)[17] and in the complex $[LNi^{II}{}_2Cl]$ (L = 1,4,7-tris(4-*tert*-butyl-2-mercaptobenzyl)-1,4,7-triazacyclononane), where adjacent octahedral *fac*-N_3S_3Ni and tetrahedral S_3NiCl sites are joined at the thiolate sulfur atoms of the hexadentate ligand (structure **iii**, R = *tert*-butyl).[15] Other mixed-valent nickel thiolate compounds are polynuclear species[39] or have not been structurally characterized.[13] In general, metal−metal distances within bioctahedral complexes containing the $M(\mu_2\text{-}SR)_3M$ core cover a wide range,[6,7] including examples in which the triple bridge is supported by a metal−metal bond.[40] In the compound examined here, the Ni···Ni separation is at 3.064(1) Å which matches quite well with the Fe···Fe distance of 3.062(4) Å found in $[(CO)_3Fe(\mu_2\text{-}SCH_3)_3Fe(CO)_3]^+$.[41] However, the rather long Ni···Ni separation and wide Ni−S−Ni angles (mean 80.16°) preclude any attraction between the metals.[42]

Spectroscopic Properties of 1−3. Infrared Spectroscopy. Since the position of the symmetric and asymmetric stretching vibrations of coordinated primary amine functions may sense variations in metal coordination number and oxidation states, compounds **1**−**3** were examined by infrared spectroscopy.[43] The observed frequencies and their assignments are listed in Table 4. Complexes **1**, **1′**, and **2** all exhibit two strong absorptions in the 3350−3200 cm^{-1} region. These were assigned to $\nu_s(NH_2)$ and $\nu_{as}(NH_2)$ stretching vibrations of the CH_2NH_2 groups. As is expected, the $\nu_s(NH_2)$ and $\nu_{as}(NH_2)$ vibrations in **2** are observed at higher frequencies than those in **1**. Here, the different N−H stretching frequencies are a result of different coordination numbers (the higher the coordination number, the longer the $M-NH_2$ bond, and the stronger the N−H bond). Relative to **1**, the higher wavenumbers in **1′** suggest coordination of the ClO_4^- counteranions in the solid state. Finally, passage from **2** to **3** causes a decrease in the frequencies of the N−H stretching vibrations. This further supports the metal-centered nature of the oxidation of $[L_3Ni_2]^+$ and the ground state of $[L_3Ni_2]^{2+}$, since the decrease in Ni−N bond lengths upon passing from $Ni^{II}-NH_2$ to $Ni^{III}-NH_2$ is expected to give a more polarized $Ni^{III}N-H$ bond, causing a weakening of the N−H bonds. The increase in the number of N−H stretching vibrations is expected for a mixed-valent $Ni^{II,III}$ species containing $Ni^{II}-NH_2$ and $Ni^{III}-NH_2$ bonds.

Table 4. Infrared Spectral ($\bar{\nu}$ (cm^{-1})), UV/Vis Spectral (λ_{max} (nm), ϵ (M^{-1} cm^{-1})), and Electrochemical Data (E (V)) for **1**−**3**

	1	**1′**	**2**	**3**
		Infrared Data[a]		
$\nu_{as}(NH_2)$	3250 s	3302 s	3320 s	3306 s, 3293 m, 3270 w
$\nu_s(NH_2)$	3193 s	3241 s	3221 s	3245 w, 3230 s
		UV/Vis Data[b]		
	312 (8482)	309 (8041)	324 (13 533)	311 (14 350)
	366 (6549)	366 (5862)	397 (2763)	391 (7144)
	502 (1186)	503 (1049)	593 (177)	473 (6753)
			922 (113)	580 (4022)
			1024 (103)	
		Electrochemical Data[c]		
$E^1_{1/2}$		+0.89 (irr)	+0.46	+0.46
$E^2_{1/2}$		+0.44	−0.02	−0.02
$E^3_{1/2}$	−0.88	−0.86		
$E^4_{1/2}$	−1.53 (irr)	−1.49 (irr)		

[a] Infrared spectra were recorded as KBr pellets (s = strong, m = medium, w = weak). [b] UV/vis spectra were recorded at 295 K. Concentrations: **1**, 1.3 × 10^{-4} M in CH_3CN; **1′**, 2.5 × 10^{-4} M in CH_3OH; **2** and **3**, 2.7 × 10^{-4} M in DMF. [c] Data recorded for **1** and **1′** in acetonitrile solution and **2** and **3** in DMF solution. All potentials are referenced to the SCE, $E^x_{1/2} = (E^{ox}_p + E^{red}_p)/2$ for reversible one-electron-transfer processes; oxidation (E^{ox}_p) or reduction peak potentials (E^{red}_p) are given for irreversible (irr) processes.

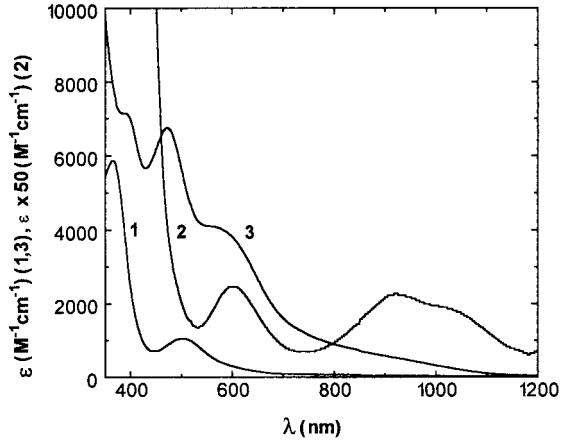

Figure 4. UV/vis spectra of **1** (in CH_3CN), **2** (in DMF), and **3** (in DMF) at 295 K. Concentrations are given in Table 4.

UV/Vis Spectroscopy. The complexes are readily identified by their UV/vis absorption spectra (Figure 4). UV/vis absorption spectra are displayed in Figure 4, and spectral data are collected in Table 4. All complexes exhibit two strong features around 312 and 366 nm (**1**, **1′**) or 391 nm (**2**, **3**), which are assigned to $\pi-\pi^*$ transitions of the ligand. The spectra of **1** and **3** are dominated by RS−Ni charge-transfer bands in the 400−800 nm region. The absorption band at 502 nm in the spectra of $[L_2Ni_2][X]_2$ (X = BPh_4^- (**1**), X = ClO_4^- (**1′**)) is typical for complexes containing planar NiN_2S_2 units.[11a] In contrast, DMF solutions of **2** absorb only weakly in the 400−1200 nm region. As is shown in Figure 4, a six-coordinate structure in solution is supported by features at 1024 and 922

(38) Franolic, J. D.; Wang, W. Y.; Millar, M. *J. Am. Chem. Soc.* **1992**, *114*, 6587−8.
(39) Krüger, T.; Krebs, B.; Henkel, G. *Angew. Chem.* **1992**, *104*, 71−2; *Angew. Chem., Int. Ed. Engl.* **1992**, *31*, 54−6.
(40) Boorman, P. M.; Patel, V. D.; Ann Kerr, K.; Codding, P. W.; Van Roey, P. *Inorg. Chem.* **1980**, *19*, 3508−11.
(41) Schultz, A. J.; Eisenberg, R. *Inorg. Chem.* **1973**, *12*, 518−25.
(42) For metal−metal bonding in D_{3h} symmetric $M(\mu_2\text{-}SR)_3M$ cores, the M−S−M angles are expected to be more acute than the 70.53° angle required for an ideal bioctahedron: Cotton, F. A.; Ucko, D. A. *Inorg. Chim. Acta* **1972**, *6*, 161−72.
(43) Nakamoto, K. *Infrared and Raman Spectra of Inorganic and Coordination Compounds*; Wiley: New York, 1978.

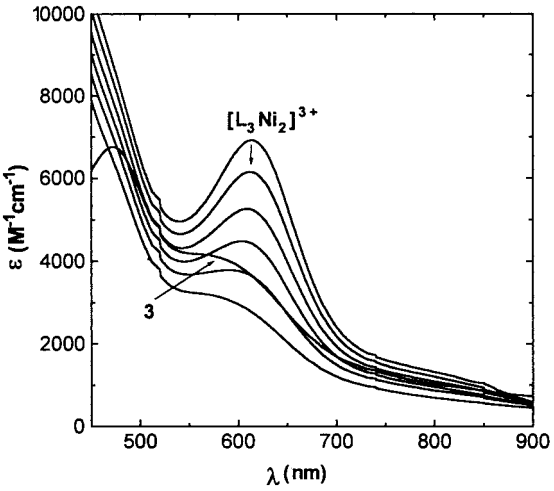

Figure 5. UV/vis spectra of $[L_3Ni_2]^{2+}$ (**3**) in DMF solution and of the transient green species $[L_3Ni_2]^{3+}$, prepared by addition of 0.5 equiv of I_2 to a solution of **3** in DMF at 295 K. Spectra for $[L_3Ni_2]^{3+}$ were recorded immediately after sample preparation. The arrow indicates the evolution of spectra recorded for the transient $[L_3Ni_2]^{3+}$ cation within 3 min intervals at 295 K. A similar evolution of UV/vis spectra is observed for electrochemically generated $[L_3Ni_2]^{3+}$.

nm which correspond to ν_1 ($^3A_{2g} \rightarrow {}^3T_{2g}$, splitting due to lower symmetry). The ν_2 band ($^3A_{2g} \rightarrow {}^3T_{2g}$) appears at 593 nm. Similar absorption spectra have been observed for other six-coordinate Ni(II) complexes with N_3S_3 or N_2S_4 donor ligands.[15,32] The absorption spectrum of **3** in DMF solution is again dominated by intense features at 473 and 580 nm which are assigned to ligand-to-metal charge-transfer transitions. The spectra taken for **3** in CD_3CN or CH_3OH solution are very similar and reveal that the positions of the two absorption bands are essentially independent of the choice of solvent.[44] The latter of these two absorptions is similar in energy as well as in intensity to the LMCT absorption in the six-coordinate Ni^{III} compound $[Ni(pdtc)_2]^-$, which has a $(d_{z^2})^1$ ground state.[32] When a solution of **3** in DMF is treated with another 0.5 equiv of oxidant (I_2 or Br_2), this feature is shifted to the more intense band at 614 nm ascribed to the LMCT absorption of the transient species $[L_3Ni_2]^{3+}$ (Figure 5).[45] Besides the intense absorption at 614 nm, the electronic absorption spectrum of this transient species reveals no further characteristic features.

Due to the absence of ligand-to-metal charge-transfer transitions in the UV/vis spectrum of **2**, the d−d transitions characteristic for octahedrally coordinated Ni^{II} ions could be observed. The intensities of these features are approximately twice as high as those in a related mononuclear $N_3S_3Ni^{II}$ complex.[15] Thus the spectrum of **2** may be considered as a simple superposition of the spectra of two mononuclear N_3S_3-Ni^{II} complexes. It is noted that strong metal−metal interactions in a dinuclear transition-metal complex may lead to drastic spectral changes of the individual ions.

One could similarly expect a superposition of the spectra of individual $N_3S_3Ni^{II}$ and $N_3S_3Ni^{III}$ ions for the spectrum of the mixed-valent species **3**. Such a situation with distinct localized Ni^{II} and Ni^{III} sites would correspond to class I in Robin and Day's classification of mixed-valence species.[46] In the other extreme (class IIIa mixed-valence species featuring strong metal−metal interactions) the properties of the component species are replaced by those of a new delocalized species. Between these two extremes lies a wide range of intermediate cases with many gradations of metal−metal interactions (class II). However, due to the intense ligand-to-metal charge-transfer transitions in the UV/vis spectrum of **3**, which would obscure any of the rather weak d−d transitions of a distinct localized $N_3S_3Ni^{II}$ ion, UV/vis spectroscopy is not suited to position compound **3** in this scale. Furthermore, an intervalence transfer (IT) band generally present in the near-IR region of the electronic absorption spectrum of a mixed-valence complex could not be observed for **3** in the region 1000−1600 nm.[47] We note that the isostructural d^5−d^6 mixed-valence $Fe^{III}Fe^{II}$ species $[L_3Fe_2]^{2+}$ exhibits a broad absorption band at λ_{max} = 1414 nm ($\epsilon \approx 1200$ M^{-1} cm^{-1}) assigned to an intervalence transition.[22]

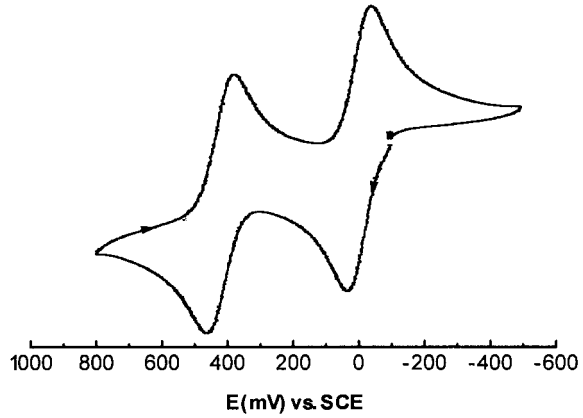

Figure 6. Cyclic voltammogram of **3** in DMF at 295 K. Experimental conditions: [**3**] ca. 1×10^{-3} M, Pt-disk working electrode, Ag wire reference electrode, 0.1 M $[Bu^n_4N][PF_6]$, scan rate = 200 mV·s^{-1}.

Electrochemistry. The redox chemistry of complexes **2** and **3** has been examined electrochemically. In the following, all redox potentials are referenced versus SCE. Table 4 summarizes the measured potentials (preliminary electrochemical data of **1** and **1′** have been included for comparative purposes).

Figure 6 displays the cyclic voltammogram of **3** in DMF solution containing 0.10 M $[Bu^n_4N][PF_6]$; that of **2** using the same experimental conditions is identical within experimental error. The CV reveals a reduction wave at $E^2_{1/2} = -0.02$ V vs SCE and an oxidation wave at $E^1_{1/2} = +0.46$ V both closely approaching the characteristics of reversible charge-transfer processes. At all scan rates (100−500 mV·s^{-1}), the ratio $i_{pc}/i_{pa} \approx 1$, $i_p/\nu^{1/2}$ is independent of scan rate, and $\Delta E^1_p = 84$ mV and $\Delta E^2_p = 73$ mV (at 100 mV·s^{-1}) increase slightly with scan rate. Controlled-potential coulometry of **3** at an applied potential of −0.3 V vs SCE in DMF solution consumed $n = 0.98 \pm 0.01$ e^-/complex (mean value of 3 determinations) and produced pale green solutions, whose UV/vis spectra are identical to that of **2**. Reoxidation at +0.2 V vs SCE caused transfer of 95% of the charge passed in reduction. The characteristics of the reduction of **3** are essentially the same as those of the oxidation of **2**. Thus, the respective one-electron-transfer processes are assigned to reduction (eq 2) and oxidation of **3** (eq 3), respectively.[48]

(44) UV/vis of **3** in CH_3CN: [**3**] = 3.0×10^{-4} M, λ_{max} = 480 nm (ϵ = 5681 M^{-1} cm^{-1}), 572 (3898). UV/vis of **3** in CH_3OH: [**3**] = 3.0×10^{-4} M, λ_{max} = 477 nm (ϵ = 7044 M^{-1} cm^{-1}), 571 (4418).

(45) The intensity of the feature at 614 nm as determined ≈20−30 s after sample preparation is characterized by an ϵ value of 6959 M^{-1} cm^{-1} (i.e., 1.7 times the value found for the 580 nm LMCT band in **3**).

(46) Robin, M. B.; Day, P. *Adv. Inorg. Chem. Radiochem.* **1967**, *10*, 247−422.

(47) (a) Allen, G. C.; Hush, N. S. *Prog. Inorg. Chem.* **1967**, *8*, 357−89. (b) Hush, N. *Prog. Inorg. Chem.* **1967**, *8*, 391−444.

$$[L_3Ni_2]^{2+} + e^- \rightleftharpoons [L_3Ni_2]^{+} \; E^1_{1/2} \quad (2)$$

$$[L_3Ni_2]^{3+} + e^- \rightleftharpoons [L_3Ni_2]^{2+} \; E^2_{1/2} \quad (3)$$

However, controlled-potential coulometry of **3** at + 0.6 V vs SCE is not as well-behaved. During electrolysis, the color of the solution changes from brown to dark green. While $n = 0.89 \pm 0.02$ e^-/complex was passed on oxidation, the reduction at +0.2 V vs SCE caused transfer of only 44% of the charge consumed in oxidation, indicating ≈50% decomposition of the oxidized species over the 30 min period of the experiment. The UV/vis spectra of the dark green solutions exhibit a transient absorption band at $\lambda_{max} = 614$ nm (Figure 5). From the decrease in ϵ_M we estimate $\tau_{1/2} \approx 15$ min (at 295 K) for the oxidized species. Thus, the one-electron oxidation of **3**, while electrochemically reversible, is chemically irreversible.

The oxidation of **2** occurs at a relatively low potential, a situation that is consistent with the observation that thiolates are powerful in stabilizing Ni in the trivalent state.[49,50] Remarkably, the redox potential for the **3**/**2** couple is quite low for a complex that has a positive charge. The majority of the complexes that exhibit potentials at or just below 0 V vs SCE are anions. The complex $[Ni(pdtc)_2]^{2-}$, for example, is oxidized at a potential of −0.085 V.[32]

We shall also consider preliminary electrochemical data for complexes **1** and **1′** that highlight the changes that occur in potentials in going from four-coordinate NiN_2S_2 to six-coordinate NiN_3S_3 complexes. Figure 7 displays the cyclic voltammograms of **1** and **1′** in acetonitrile and methylene chloride solution.

In the potential range +1.2 V to −1.7 V vs SCE, acetonitrile solutions of **1′** display a reversible reduction wave at $E^3_{1/2} = -0.86$ V ($\Delta E^3_p = 79$ mV), a quasi-reversible oxidation wave at $E^2_{1/2} = +0.44$ V ($\Delta E^2_p = 79$ mV), and irreversible oxidation and reduction waves at $E^1_{1/2} = +0.89$ V and $E^4_{1/2} = -1.49$ V, respectively. The cyclic voltammogram of **1** (in the cathodic potential region) is similar to that of **1′**. For now, we note that the reductions of **1** and **1′** (at $E^3_{1/2}$) occur at potentials that are quite comparable to Ni^{II}/Ni^{I} reduction potentials of $NiN_2(\mu_2\text{-}SR)_2$ complexes. For example, the trimetallic compound $[(NiL)_2Ni]Cl_2$ (L = 1,5-bis(mercaptoethyl)-1,5-diazacyclooctane)[51] undergoes a one-electron reduction at −0.77 V vs SCE ascribed to the formation of Ni^{I}.[52] Similarly, the oxidations of **1** and **1′** (at $E^2_{1/2}$) occur at potentials that are close to the $E^1_{1/2}$ value found for **3**.

Under the assumption that these processes correspond to metal-centered reduction and oxidation, the passage from four-coordinate NiN_2S_2 in **1** to six-coordinate NiN_3S_3 coordination units in **3** results in a further stabilization of the Ni^{III} state by ≈−0.46 V. Also pertinent to these results are the electrochemical properties of the recently reported dithiolate-bridged dinickel(II) complexes $[Ni_2L]^{2+}$ (L represents the 2 × 2 condensation product of 2,6-diformyl-4-methylthiophenol and 1,3-ethylenediamine). The complexes have been reported to undergo two reversible reductions at $E_{1/2} = -1.18$ V and −0.70 V vs SCE, one reversible oxidation at $E_{1/2} = +0.95$ V, and one quasi-reversible oxidation at $E_{1/2} = +1.36$ V.[13e,f] The more positive oxidation potentials in these latter species indicate a destabilization of the Ni^{III} state, while the more positive reduction potentials indicate an easier access to the Ni^{I} state. This is consistent with the observation that imine type ligands, due to their π acceptor properties, may stabilize metals in low formal oxidation states.

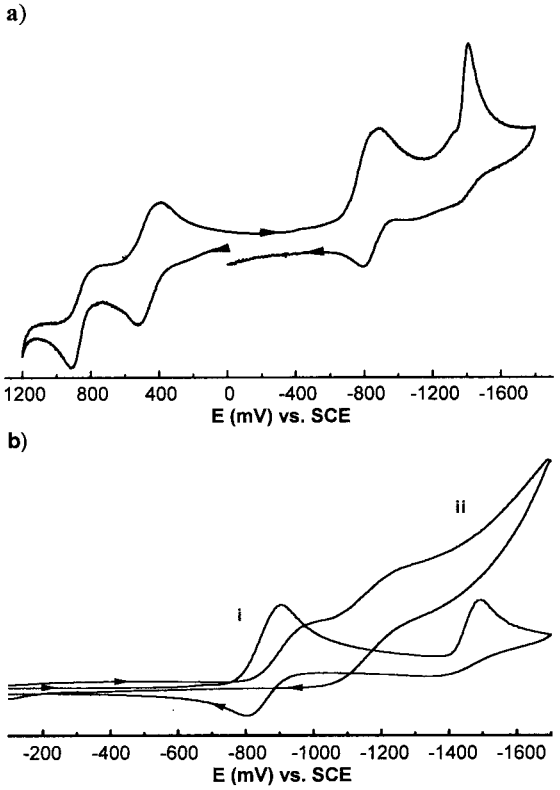

Figure 7. (a) Cyclic voltammogram of **1′** in CH_3CN at 295 K. (b) Cyclic voltammogram of **1** in CH_3CN (i) and CH_2Cl_2 (ii) at 295 K. Experimental conditions: [**1′**], [**1**] ca. 1×10^{-3} M, Pt-disk working electrode, Ag wire reference electrode, 0.1 M $[Bu^n_4N][PF_6]$, scan rate = 200 mV·s^{-1}.

EPR Spectroscopy. The mixed-valent nature of **3** has been further confirmed by preliminary EPR measurements. The EPR spectrum of a powdered sample of **3** at 77 K is shown in Figure 8. The g values $g_{||} = 2.09$ and $g_{\perp} = 4.0$ taken from the spectrum are characteristic for a system with spin $S = {}^3/_2$ in a nearly axial environment with a high zero-field splitting (compared to the $h\nu$ energy of the microwave). In this case $g_{||} \approx 2$, $g_{\perp} \approx 2(S + {}^1/_2) = 4$ for $S = {}^3/_2$.[53] EPR investigations on single crystals confirm this result. It should be noted that at temperatures slightly above 80 K the low-field signal at $g \approx 4$ disappears in favor of a signal near g ≈ 2, indicating another coupling scheme.

It is unlikely that the $S = {}^3/_2$ ground state of **3** results from uncoupled high-spin Ni^{III} ($S = {}^3/_2$) and low-spin Ni^{II} ($S = 0$)

(48) K_{com} is calculated to be 1.4×10^8, showing negligible disproportionation of **3**. $K_{com} = \exp(nF(\Delta E/RT)$, where $\Delta E = |E^1_{1/2} - E^2_{1/2}|$. The CV data are indicative of some degree of metal−metal interaction. If the metal ions behave as independent and identical atoms, the separation in potentials and comproportionation constant will have the statistical values of $E_1 - E_2 = (2RT/F)\ln 2 = 36$ mV (298 K) and $K_{com} = 4$ (298 K).

(49) (a) Krüger, H.-J.; Holm, R. H. *Inorg. Chem.* **1987**, *26*, 3645−7. (b) Krüger, H.-J.; Peng, G.; Holm, R. H. *Inorg. Chem.* **1991**, *30*, 734−42.

(50) Fox, S.; Wang, Y; Silver, A.; Millar, M. *J. Am. Chem. Soc.* **1990**, *112*, 3218−20.

(51) Musie, G.; Farmer, P. J.; Tuntulani, T.; Reibenspies, J. H.; Darensbourg, M. Y. *Inorg. Chem.* **1996**, *35*, 2176−83.

(52) Cyclic voltammetry of **1** in CH_2Cl_2 solution leads to complete loss of the anodic current for the couple at $E^3_{1/2}$. This is probably due to reduction of the solvent. Similar effects have been observed for solutions containing electrochemically generated mononuclear Ni^{I} species and alkyl halides: Efros, L. L.; Thorp, H. H.; Brudwig, G. W.; Crabtree, R. H. *Inorg. Chem.* **1992**, *31*, 1722−4.

(53) Pake, G. E.; Estle, T. L. *The Physical Principles of Electron Paramagnetic Resonance*, 2nd ed.; W. A. Benjamin Publ.: London, 1973; p 127.

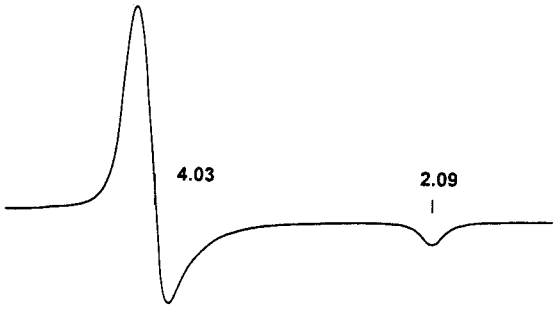

Figure 8. EPR powder spectrum (9 GHz) of $[L_3Ni_2][BPh_4]_2 \cdot MeOH$ (**3**) at 77 K. Apparent *g* values are indicated.

ions. A situation in which a low-spin Ni^{III} ($S = {}^1/_2$) is ferromagnetically coupled to Ni^{II} ($S = 1$) seems to be more likely. This follows from the UV/vis data of **2**, which indicate $S = 1$ for octahedral Ni^{II} in **2** or **3**. The Ni^{III} ions in **3** are considered to be low-spin since a mononuclear Ni^{III} complex containing a N_4S_2 donor set has been reported to be low-spin, and even in cases of rather weak ligands such as the fluoride ion in K_3NiF_6 are the Ni^{III} ions low-spin configurated.[54] Unfortunately, a hyperfine coupling to nitrogen atoms (^{14}N) of the ligand, which could have helped characterize the spin coupling present, could not be observed in the EPR powder and single-crystal spectra. EPR spectra of frozen DMF solutions also do not reveal hyperfine coupling. Nitrogen hyperfine coupling has been observed in an octahedral $N_2S_4Ni^{III}$ complex;[32] however, other complexes containing nitrogen atoms bound to Ni^{III} have been reported to exhibit unresolved EPR signals. In this case, the presence of hyperfine coupling was suggested by a rather broad EPR signal.[30] The broad EPR signals of the compound examined here can probably also be attributed to unresolved ^{14}N hyperfine interactions of the electronic spin system with the nitrogen atoms of the ligand.

(54) Reinen, D.; Friebel, C.; Propach, V. *Z. Anorg. Allg. Chem.* **1974**, *408*, 187−204.

It is interesting to note that an intramolecular ferromagnetic exchange interaction is also observed in the linear trinuclear complex $Ni_3(acac)_6$.[55] This complex features a central $O_3Ni(\mu_2\text{-}O)_3Ni(\mu_2\text{-}O_3)NiO_3$ core in which adjacent NiO_6 polyhedra are arranged in a face-sharing fashion similar to that in **2** and **3**. We anticipate a more detailed study of the electronic spin systems of **2** and **3** by magnetic susceptibility measurements and ^{61}Ni Mössbauer spectroscopy.

Summary. The main findings of the present work are summarized as follows. (1) The ability of the coordinatively unsaturated complex **1** to bind exogenous ligands has been demonstrated by the synthesis and characterization of the four- and six-coordinate nickel thiolate complexes **1** and **3**. (2) The mixed-valent compound **3** features a unique, bioctahedral $N_3Ni(\mu_2\text{-}SR)_3NiN_3$ core, as well as a robust $Ni^{II,III}$ thiolate system. (3) Complex **3** in the solid state is a trapped-valence compound that is characterized by a $S = {}^3/_2$ spin state below $\approx$80 K. (4) Passage from four-coordinate NiN_2S_2 to six-coordinate NiN_3S_3 complexes results in easing the accessibility of the Ni^{III} state. Current efforts in these laboratories focus on the preparation and characterization of dinuclear complexes of composition $[N_2Ni(\mu_2\text{-}SR)_2(\mu_2\text{-}S)NiN_2]^{n+}$ (i.e., one ligand HL is replaced by S^{2-}).

Acknowledgment. This work was supported by the Deutsche Forschungsgemeinschaft. B.K. thanks Prof. Dr. H. Vahrenkamp for his generous support. We also thank Prof. Dr. B. Krebs (University of Münster) for the use of the STOE-IPDS diffractometer and are indebted to Dipl. Chem. I. Jolk and B. Müller for help in collecting the X-ray data.

Supporting Information Available: X-ray crystallographic files for **1** and **3**, in CIF format, are available on the Internet only. Access information is given on any current masthead page.

IC980131P

(55) (a) Ginsberg, A. P.; Martin, R. L.; Sherwood, R. C. *J. Chem. Soc., Chem. Commun.* **1967**, 856−8. (b) Ginsberg, A. P.; Martin, R. L.; Sherwood, R. C. *Inorg. Chem.* **1968**, *7*, 932−6. (c) Boyd, P. D: W. Martin, R. L. *J. Chem. Soc., Dalton Trans.* **1979**, 92−5.